

Protection of high density polyethylene/silicon composites from UV/VIS photo-degradation

L. Santonja-Blasco^{1,2}, I. Rodriguez³, S. Sanchez-Ballester¹, J. D. Badia^{1,4}, F. Meseguer^{3,*}, A. Ribes-Greus^{1,*}

This is an open-access version, according to <http://www.sherpa.ac.uk/romeo/issn/0021-8995/>

Full text available at <http://onlinelibrary.wiley.com/doi/10.1002/app.45439/abstract>

DOI: <https://doi.org/10.1002/app.45439>

Please, cite it as:

L. Santonja-Blasco, I. Rodriguez, S. Sanchez-Ballester, J. D. Badia, F. Meseguer, A. Ribes-Greus. Protection of high density polyethylene/silicon composites from UV/VIS photo-degradation. Journal of Applied Polymer Science 2017;134(43): 45439

¹Instituto de Tecnología de los Materiales (ITM), Universidad Politècnica de València (UPV), Camí de Vera S/N, 46022 Valencia, Spain.

²FAMU/FSU College of Engineering, Chemical and Biomedical Engineering Department, 2525 Pottsdamer St., Tallahassee, FL 32310-6046, USA

³Instituto de Tecnología Química (ITQ), Centro Mixto Consejo Superior de Investigaciones Científicas / Universitat Politècnica de València (CSIC / UPV), Avenida de Los Naranjos, s/n, 46022 Valencia, Spain

⁴Departament d'Enginyeria Química. Escola Tècnica Superior d'Enginyeria. Universitat de València. Av. de la Universitat, s/n, 46100, Burjassot, Spain.

*Corresponding authors:

F. Meseguer fmese@fis.upv.es
A. Ribes-Greus aribes@ter.upv.es

Protection of high density polyethylene/silicon composites from UV/VIS photo-degradation

L. Santonja-Blasco^{1,2}, I. Rodriguez³, S. Sanchez-Ballester¹, J. D. Badia^{1,4}, F. Meseguer^{3,*}, A. Ribes-Greus^{1,*}

ABSTRACT

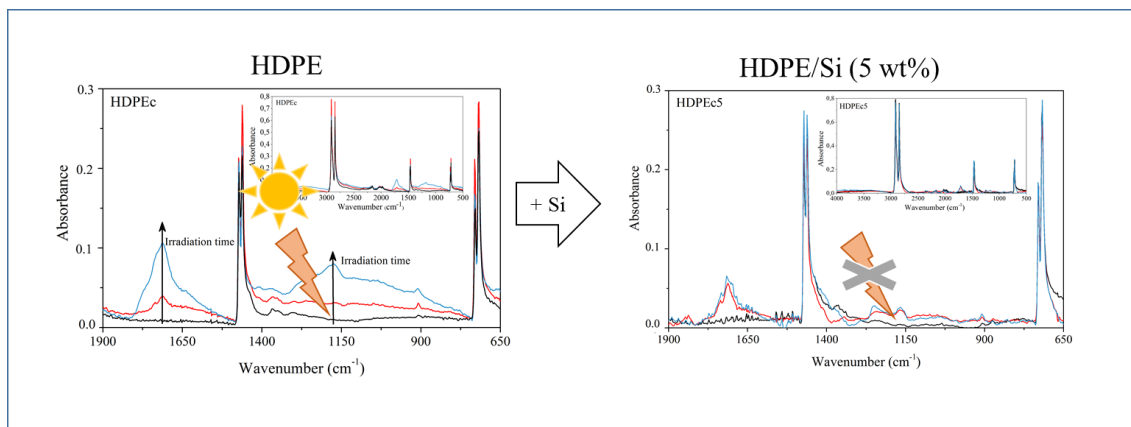
The extent of the ultraviolet/visible (UV/VIS) photo-irradiation effect on high-density polyethylene (HDPE) and HDPE/Si composites is reported in terms of the addition of silicon (Si) microparticles at contents of 0.1, 1 and 5 wt%. A standard accelerated UV/VIS exposure is applied during 2750 h, corresponding to 22 months in Florida, USA. Thermogravimetry, Differential Scanning Calorimetry and Fourier-Transform Infrared Spectroscopy stand out as reliable techniques to monitor the quality of HDPE/Si composites. The increasing addition of Si microparticles delayed the photo-degradation of HDPE/Si composites. Due its strong light scattering effect, Si microparticles blocks the degradation of tertiary carbons of the HDPE backbone reducing the apparition of vinyl groups, which prevents the structural impoverishment of HDPE/Si composites. Consequently, the variation of the crystallization and melting temperatures, which are indicators of photo-degradation, were not modified. In general, the formulation of HDPE/Si composites with a 5 wt% of Si microparticles was useful to protect the material from photo-degradation, thus being an environmentally friendlier reliable alternative UV/VIS blocker.

KEYWORDS: high-density polyethylene HDPE, Silicon (Si) microparticles, composite; photo-chemical degradation

HIGHLIGHTS

- The light scattering effect of Si microparticles is shown in HDPE/Si composites
- Si prevented from vinyl formation due to photo-degradation of HDPE
- The mass-loss of thermal decomposition was reduced by the addition of Si
- HDPE/Si composites with a 5 wt% of Si increased the thermal stability
- HDPE/Si composites with a 5 wt% of Si retained the crystallization behaviour

GRAPHICAL ABSTRACT



1. INTRODUCTION

Polyolefins are the polymers with the largest volume market due to their excellent mechanical and thermal properties, among others.¹ Polyethylene (PE) is extensively produced in many different grades as well as in co-polymer grade by changing the type and content of the co-monomer, for covering numerous applications.² It is well stated that polyolefins may degrade due to external factors such as sun-light irradiation, temperature and humidity at outdoor applications.³⁻⁵ Wavelengths in the range between 280 and 800 nm have sufficient energy to cause a cleavage of the chemical structure of the polymer.^{6,7} Photo-oxidation in polyolefins takes place when free radicals are generated through energy transfer mainly at chromophores, double bonds of the polymer or catalyst residues.⁸⁻¹² The synergetic effect of ultraviolet/visible (UV/VIS) radiation in presence of oxygen changes the initial polymer chemical structure,¹³ which consequently influences the mechanical and thermal properties.¹⁴

The control of the effects of oxidation by the incorporation of light blocking additives is key to protect the chemical structure of the polymer and design materials that ensure long-term properties.¹⁵⁻¹⁸ The protection of the polymers against UV/VIS photo-irradiation is still a current issue despite the extended use of organic and inorganic UV blockers.¹⁹⁻²⁸ The advantage of inorganic particles is their stability against UV photo-irradiation. In addition, the high refractive index produces back-diffraction of the radiation and, therefore, they play the role of a mirror for UV light. In contrast, the organic scavengers are used as sacrificial elements, which therefore degrade upon UV radiation.

Silicon (Si) microparticles stand out as added-value additives for many sectors. Previously, Si microparticles with uniform size and shape and high refractive index have been found to behave as strong light scatterers able to block irradiation in the mid and far infrared range.^{29,30} Besides, polydispersed Si microparticles represent an environmentally friendly alternative to conventionally used chemical and physical solar protectors, such

as TiO_2 , ZnO and Al_2O_3 ,³¹ which are currently developed in the field of cosmetics and pharmaceuticals.^{32,33} Si microparticles may act as protectors of sunlight radiation in applications such as adhesives, protective coatings, composites or microelectronics.³⁴ Therefore, due to the width and volume of the market of polyolefins such as polyethylene, in particular at applications which service outdoor, the inclusion of Si microparticles in the catalogue of sunlight protectors may represent a relevant impact in the market.

Thermal analysis techniques based on changes in the crystallization and melting behaviour and on the thermal decomposition of polymers have been used to test the degradation of polymers.³⁵⁻³⁷ From a technological point of view, Differential Scanning Calorimetry (DSC) and Thermogravimetric Analysis (TGA) stand out as fast and high sensitivity instruments to detect changes due to degradation.³⁸⁻⁴⁰ In particular, sensible parameters as the crystallization and melting temperature peaks and the mass-loss of the main decomposition peak can be used to correlate the potential preventive effect towards sunlight degradation with the amount of Si present in the HDPE/Si composites. A first attempt reported by Gil-Castell et al. showed preliminary promising results about the effects of silicon microparticles on the durability of raw polypropylene against UV/VIS degradation.⁴¹ This paper proposes a step further showing the validity of Si microparticles to protect commercial polyethylene, to widespread the use of Si microparticles to preserve polyolefins from sunlight irradiation.

Summing up, the aim of this work is ~~was therefore~~ to assess the effect of the addition of Si microparticles (0.1, 1 and 5 wt.%) to protect high-density polyethylene from UV/VIS photo-irradiation, by means of thermal, morphological and structural analysis. The chemical structure as well as the thermal properties studied before and after irradiation of the composites containing different amounts of Si microparticles indicated a protective

effect against photo-degradation up to, at least, 22 months, for the HDPE/Si composites with 5% wt. of Si.

2. EXPERIMENTAL

2.1. Material and sample preparation

Commercial high density polyethylene (HDPE) Dow TM 25055EE (density of $0.953 \text{ kg}\cdot\text{m}^{-3}$ at 23.3°C) was used as matrix. Polydispersed silicon microparticles with size below $2.3 \mu\text{m}$ (98%) obtained after grinding and screening processes of metallurgical grade silicon powder (Silgrain®, 99.5% purity from Elkem) were used as fillers. The addition of Si into HDPE was performed at 0.1, 1 and 5 wt%. In order to improve the compatibility between matrix and filler, a coupling agent of polyethylene-grafted-maleic anhydride (PEgMA) *Fusabond® E MB226DE*, supplied by DuPont, was added in a 1:3 (wt/wt) Si:PEgMA proportion. The three components were blended in a Haake Polylab mixer at 158°C during 15 minutes. Films of $200 \mu\text{m}$ were prepared in a press by compression melt at 158°C and quenched to room temperature. Several specimens were cut from films for further durability tests by UV/VIS photo-irradiation. The composites were labelled as HDPEcX, being c the compatibilizer and X the mass percentage of Si microparticles, as HDPEc, HDPEc0.1, HDPEc1 and HDPEc5.

2.2. Accelerated UV/VIS photo-irradiation tests

The UV/VIS photo-irradiation of composites was carried out by using an accelerated exposure system according to the standardised ISO4892-Method A.⁴² A Suntest XLS+ (Chicago, IL, USA) that uses a Xenon lamp with a solar standard filter, which cuts the wavelengths (λ) below 290 nm in order to simulate the UV/VIS spectrum, was used. The UV/VIS photo-irradiation time in the exposure system was converted to the approximated real sun exposure time reference in Jacksonville, Florida (USA) with an annual total radiant energy of $5800 \text{ MJ}\cdot\text{m}^{-2}$ ($\lambda = 280$ to 3000 nm), corresponding to $3248 \text{ MJ}\cdot\text{m}^{-2}$ in

the range of $\lambda = 280$ to 800 nm.^{41,43} The hours of photo-irradiation, the total radiant energy for that time and the corresponding outdoor exposure times are given in **Table 1**.

Table 1. Correlation of the hours of radiation in the Suntest, the total radiant energy and the approximated real outdoor exposure times for Jacksonville, Florida (USA)

Suntest exposure (hours)	Energy (MJ·m⁻²)	Approximated real exposure (months)
750	1620	6.07
1250	2700	10.11
2000	4320	16.18
2750	5940	22.25

2.3. Analytical characterisation

2.3.1. Scanning Electron Microscopy (SEM)

Scanning Electron Microscopy (SEM) analyses were used to verify the well dispersion of the microparticles in the polymers. SEM images of the composites were taken at accelerating voltages of 20kV on a Jeol 6300 microscope after covering the samples with a gold thin film by sputtering. Samples were cut perpendicularly to the lamellar direction after being plunged in liquid nitrogen for few seconds.

2.3.2. Thermogravimetry

The thermo-oxidative stability of HDPE and HDPE/Si composites submitted to a standard accelerated UV/VIS photo-irradiation was assessed by Thermogravimetric analysis in a Mettler Toledo TGA/SDTA 851 (Columbus, OH, USA). The international standard described in the ISO11358 was followed.⁴⁴ The sample was heated at 10 °C/min from 0 °C to 800 °C under oxidative atmosphere (O₂ flow 100 mL·min⁻¹) to obtain the thermograms and the characteristic temperatures of the thermo-oxidative decomposition

process. All experiments were performed by triplicate and the averages were taken as representative values.

2.3.3. Differential Scanning Calorimetry

The evolution of morphology and thermal properties of the HDPE/Si composites was monitored by differential scanning calorimetry (DSC), measured by means of a Mettler Toledo DSC 822 (Columbus, OH, USA). The methodology described in the international standard ISO11357 was used.⁴⁵ Three calorimetric scans were carried out to each sample from -60 to 200°C at a heating/cooling/heating rate of 10°C/min under N₂ flow (50 mL·min⁻¹). Specimens of ~5 mg were introduced in a pierced aluminium crucible, with capacity for 40 µL. All experiments were performed by triplicate and the averages were taken as representative values.

2.3.4. Fourier Transform Infrared Spectroscopy (FT-IR)

Fourier Transform Infrared Spectroscopy (FT-IR) was used to characterize the structure of neat films of HDPE and HDPE/Si composites by following the progress of the frequency bands associated with the chemical functional groups formed during the UV/VIS photo-irradiation of samples. The FT-IR spectra were obtained using a Thermo Nicolet 5700 spectrometer (Thermo Fisher Corporation, MA, USA), in the 400 to 4000 cm⁻¹ region, with a 4 cm⁻¹ resolution, and using an Attenuated Total Reflectance (ATR) modulus. In order to obtain accurate results, 64 scans were performed at 3 locations on the sample.

3. RESULTS AND DISCUSSION

3.1. Spectroscopic evaluation of the matrix

The characteristic FT-IR band of HDPE is shown in **Figure 1**. Common additives for polyolefins⁴⁶ such as talc for increasing rigidity (1017 cm⁻¹), Irganox 1010 as antioxidant (1740 cm⁻¹), calcium as nucleation agent (1540 cm⁻¹) or sorbitol-based as clarifier (OH

band region $\sim 3400\text{ cm}^{-1}$) were not present, and therefore the impact of Si microparticles to protect the HDPE/Si composites from photo-irradiation was analyzed without interferences.

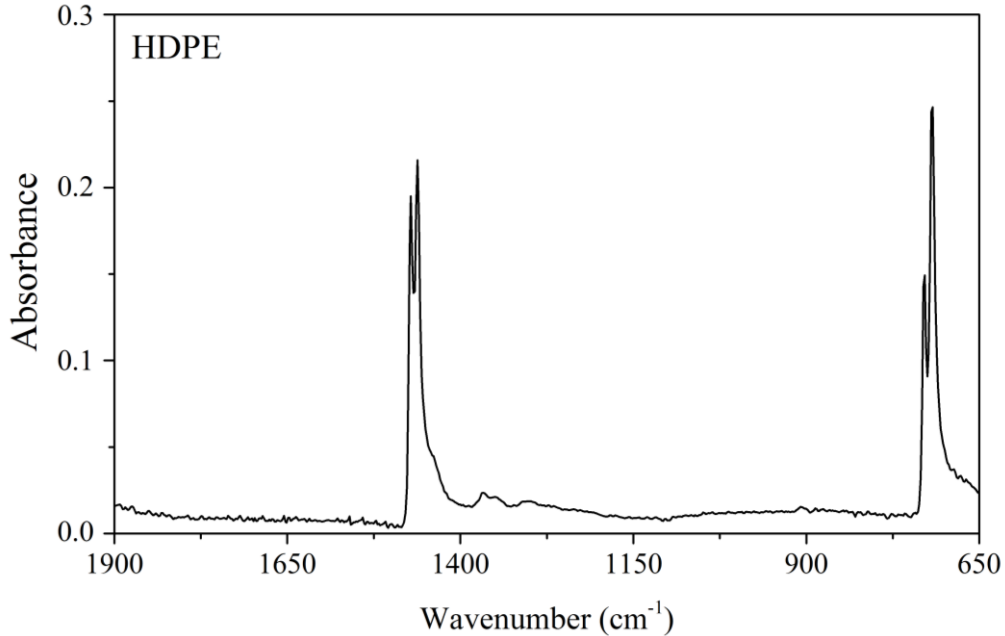


Figure 1. FT-IR spectrum of HDPE

3.2. Dispersion of Si microparticles into the HDPE/Si composites

A well dispersion of the Si microparticles in the HDPE matrix is required to ensure homogenous protection through the surface and the bulk. The compatibility and improvement of interfacial adhesion between both components was guaranteed by the use of the coupling agent,⁴⁷⁻⁴⁹ which ensured the dispersion of Si microparticles in the HDPE matrix, as shown by the SEM images of **Figure 2**, where the Si microparticles appear as white spots into the polymer matrix. Micrographs with different magnifications are presented with the aim to show the Si microparticles integration into the polymer as well as the long range well-dispersion.

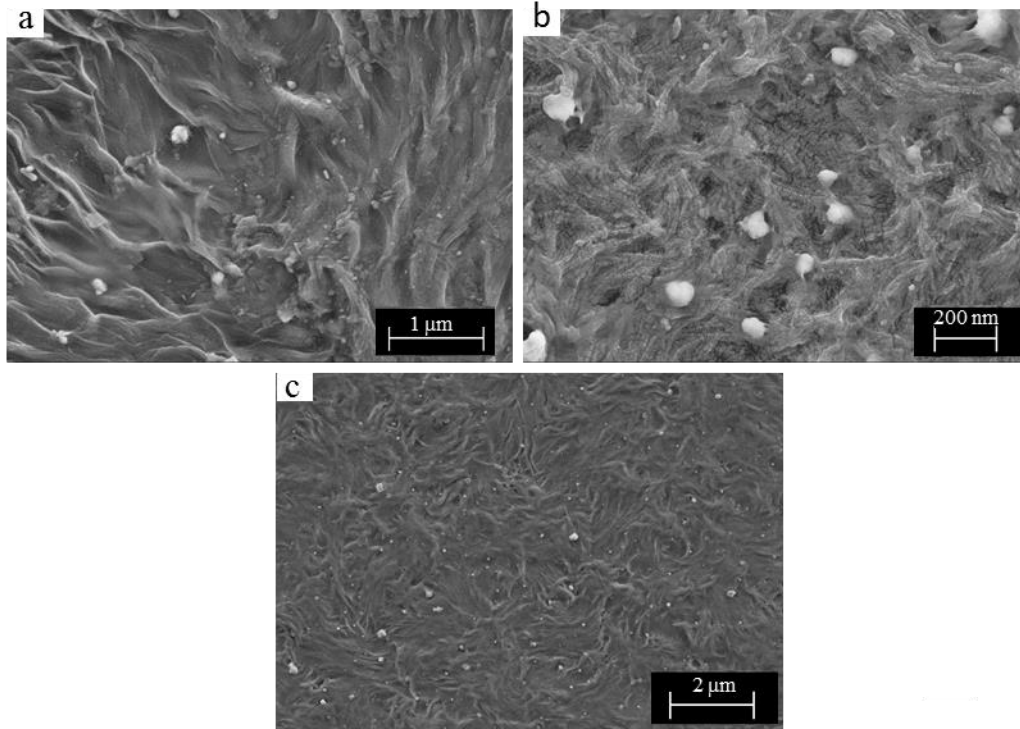


Figure 2. SEM images of HDPE polymer modified with coupling agent (HDPEc) and several amounts of silicon microparticles. a) HDPEc0.1 b) HDPEc1 and c) HDPEc5. Note that the bright spots represent Si microparticles dispersed into the HDPE matrix.

3.3. Macroscopic effects of UV/VIS photo-irradiation

The physical aspect of the probes of HDPE, HDPE with coupling agent and HDPE/Si composites subjected to different UV/VIS photo-irradiation times is shown in **Figure 3**. The colour of the samples changed from transparent to dark brown by the addition of Si microparticles and therefore their application should be focused in sectors with no specific requirements of transparency. After the first stage of photo-irradiation (750 hours), the samples with none or low content of Si (0 and 0.1 wt.%) turned into yellow, became fragile and some of them broke. Note that, even broken, further analysis of fragments was interesting to monitor the effects of photo-irradiation on structure, morphology or thermal properties. In contrast, HDPE/Si composites with high Si content (1 and 5 wt.%) after 750 h of photo-irradiation were visually very similar to their corresponding non-irradiated samples. However, these composites became quite brittle

after 2000 hours of photo-irradiation. The physical stability and handling of HDPE/Si composites was enhanced by the increase of the Si content to 5 wt.%. Only HDPEc5 remained in one piece after 2750 hours of photo-irradiation.












Samples	Irradiation time				
	non-irradiated	750 hours	1250 hours	2000 hours	2750 hours
HDPEc					broken
HDPEc0.1					broken
HDPEc1					broken
HDPEc5					

Figure 3. Macroscopic effects of photo-irradiation on HDPE/Si composites

3.4. Thermal stability of photo-irradiated HDPE/Si composites

The control of polymer degradation is a goal for many companies that pursue robust outdoor resistant products based on polyethylene. In this section, the effects of UV/VIS photo-irradiation on HDPE and HDPE/Si composites were assessed in terms of thermal stability. The thermogravimetric thermograms (TG) and first-derivative thermograms (DTG) of HDPE, the coupling agent PEGMA, HDPE with coupling agent (HDPEc) and the HDPE/Si composite with a 1 wt% of Si (HDPEc1) are shown in **Figure 4 a-d**. The rest of HDPE/Si composites are not shown for the sake of conciseness.

HDPE showed three main decomposition regions (**Figure 4a**). The first decomposition stage from 225 °C to 375°C, with peak at 300 °C, that comprised a 15-20% of the total mass loss, was related to the volatilization of the low molar mass molecules and oxidation

products.⁵⁰ Subsequently, the main cleavage of polyethylene chains occurred from 375°C to 470°C, with peak at 425°C. Finally, during the highest temperature mass-loss stage, the complete volatilization of the oxidized sample occurred. The mechanism of thermo-oxidative decomposition is well reported and starts with the formation of radicals groups, acting as precursors of a complex process that dramatically reduced the molar mass of the original sample.⁵¹⁻⁵³ As expected, the thermal decomposition of commercial HDPE with oxygen showed a pattern⁵⁴ which is more complex than that shown under inert atmosphere, where just a peak at 485°C at 10 °C·min⁻¹ is usually found.⁵⁵ Complex decomposition steps were also discussed by Camacho *et al.* for polyolefins,⁵⁶ in terms of the formation of peroxy radicals and hydroperoxides, being converted into other labile products.

The thermogram of the coupling agent showed a single mass-loss decay centred at 525 °C (**Figure 4b**) and, in combination with HDPE, presented a more heterogeneous DTG curve due to the interaction of the components and degradation during the mixing process (**Figure 4c**). Finally, the thermo-decomposition process of HDPEc1 (**Figure 4d**) ranged from 380 to 500°C, with alike main peaks as those displayed by HDPEc. The rest of HDPE/Si composites, as shown in **Figure 5 a-d**, exhibited similar profiles.

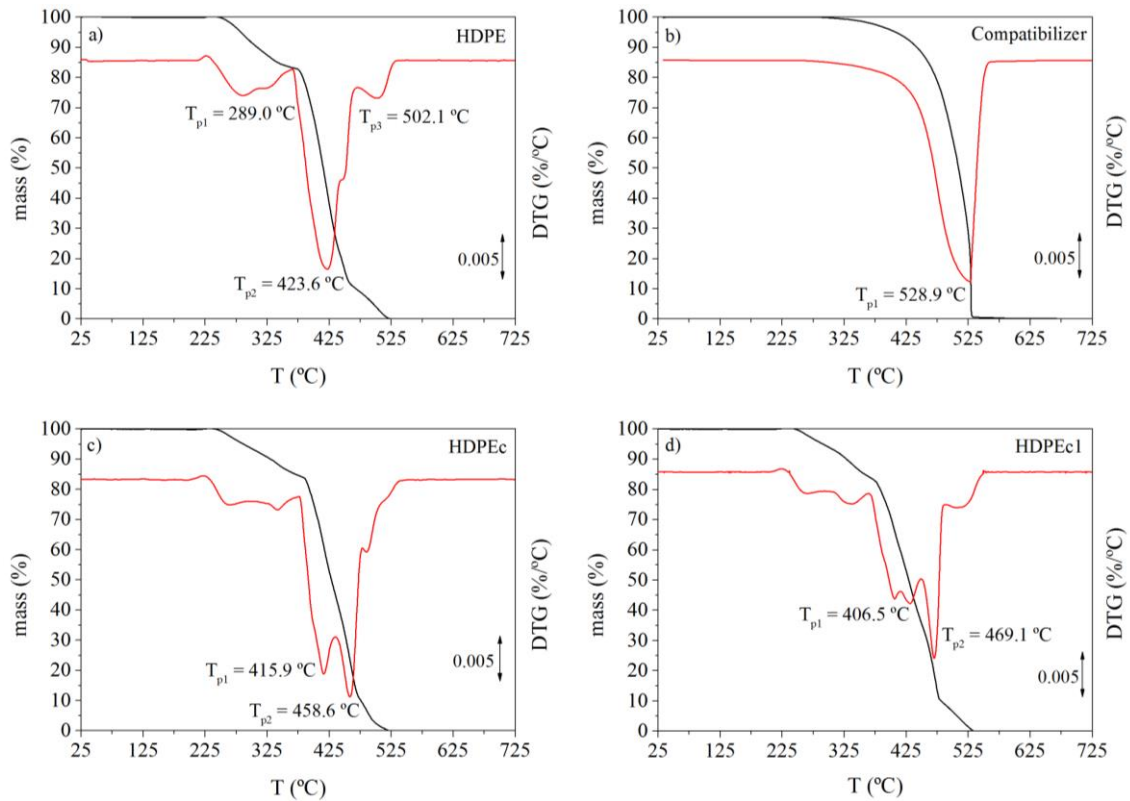


Figure 4. TG-DTG thermograms for a) HDPE, b) coupling agent, c) HDPEc and d) HDPEc1

The TG and DTG thermograms of the HDPE/Si composites subjected to the highest photo-irradiation stage, i.e. 2750 h, are displayed in **Figure 5** a-d. As the content of Si microparticles increased, the decomposition thermogram of the sample was more heterogeneous, as demonstrated by the appearance of small peaks. The peak decomposition temperatures (T_p) of the main mass-loss stages appeared for HDPEc0.1 at ~ 424 , 444 and $469\text{ }^{\circ}\text{C}$; for HDPEc1 at ~ 433 and $470\text{ }^{\circ}\text{C}$; and for HDPEc5 at ~ 425 and $479\text{ }^{\circ}\text{C}$. The T_p of the highest mass-loss stage of HDPE/Si composites was displaced to higher values when increasing Si content, from $\sim 469\text{ }^{\circ}\text{C}$ with 0 and 0.1 wt.% of Si towards $\sim 479\text{ }^{\circ}\text{C}$ with 5 wt.% of Si.

The high heterogeneity of the decomposition profiles may complicate the quantitative monitoring of the stabilisation in terms of the main decomposition peaks or the onset temperature of the first step of decomposition.^{57,58} Actually, no significant changes were observed in the onset temperature of the HDPE/Si composites after photo-irradiation.

However, the mass-loss of the main decomposition peak stands out as a reliable parameter to be used as a macroscopic indicator of the degradation. In this sense, the stability of HDPE/Si composites subjected to UV/VIS photo-irradiation is shown in **Figure 6** in terms of the mass-loss in the decomposition region from ~225 to 375°C. The values next to arrows represent the relative mass-loss reduction (*RML*) between neat and photo-irradiated samples, calculated as $(|\%m_{0h} - \%m_{2750h}| \cdot \%m_{0h}^{-1}) \cdot 100$. The *RML* was enhanced from a 52% for HDPEc down to a 25% for HDPEc0.1, a 13 % for HDPEc1 and only a 6% for HDPEc5.

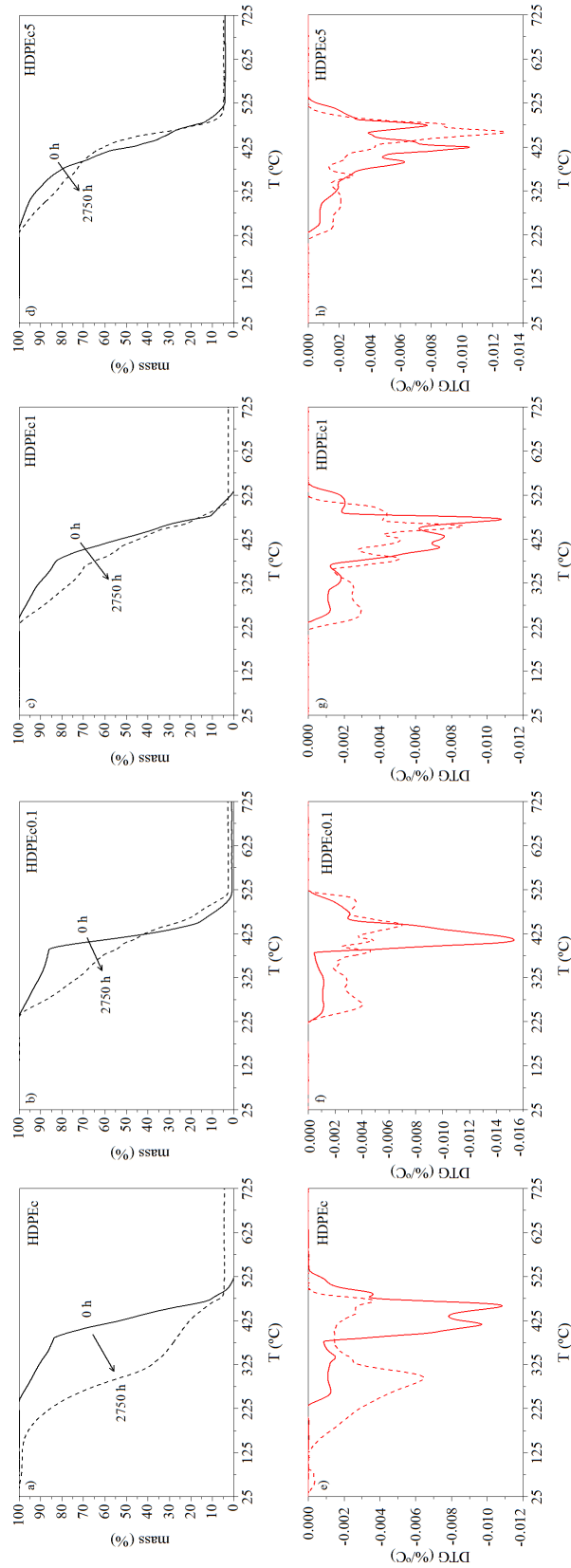


Figure 5. TG (up) and DTG (down) thermograms of a,e) HDPEc, b,f) HDPEc0.1, c,g) HDPEc1 and d,h) HDPEc5 at 0h (solid line) and 2750 h (dashed line) of photo-irradiation.

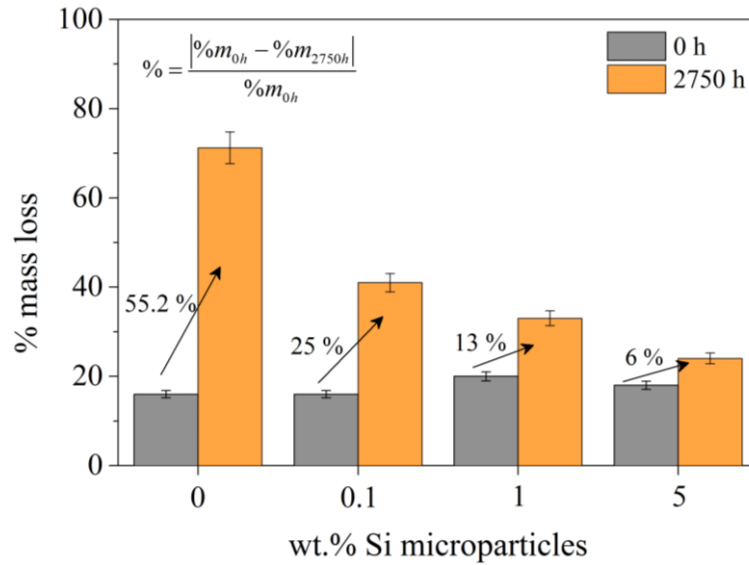


Figure 6. Mass-loss and relative mass reduction (percentage written in the arrows) observed during the thermo-decomposition of the samples irradiated 0h and 2750h versus the weight percent of silicon microparticles. Region of decomposition (~225 to 375°C)

3.5. Effect of UV/VIS photo-irradiation on the thermal properties of HDPE/Si composites

The thermal properties of HDPE/Si composites subjected to UV/VIS photo-irradiation were monitored by means of differential scanning calorimetry, which stands out as a reliable thermal analysis technique to ascertain the degree of quality of polymers during service life or after a certain degradation period.⁵⁹⁻⁶⁵ In order to set the base scenario for further assessment of sunlight protection, the comparative plots of the endotherms and exotherms experimentally obtained for HDPE, the coupling agent, HDPEc and HDPE/Si with a 1 wt.% of Si (HDPEc1) are shown in **Figure 7**. For the sake of conciseness, the latter sample is shown as model case, whereas the response of the rest of HDPE/Si composites is shown in **Figure 8**.

The thermal behaviour of the coupling agent was overlapped by the main thermal transitions of HDPE (Figure 7a and b). The coupling agent seemed to act as nucleant agent (Figure 7c), accelerating the non-isothermal crystallization rate by increasing the

crystallization temperature (T_c) and the melting enthalpy of the HDPE, albeit the onset temperature of the crystallization did not significantly change ($\sim 120^\circ\text{C}$). Similarly, the addition of Si microparticles accelerated the crystallization process by slightly shifting T_c towards higher temperatures (Figure 7d) due to a nucleation effect of the Si microparticles, as also reported for composites made of HDPE and silica.^{66,67} The melting enthalpy did not significantly change after adding Si microparticles, and remained at ranges between 175-190 J·g⁻¹.

In order to assess the influence of the content of Si microparticles on the photo-chemical protection of HDPE/Si in terms of thermal properties the comparative plots of the endotherms and exotherms as a function of degradation time are shown in

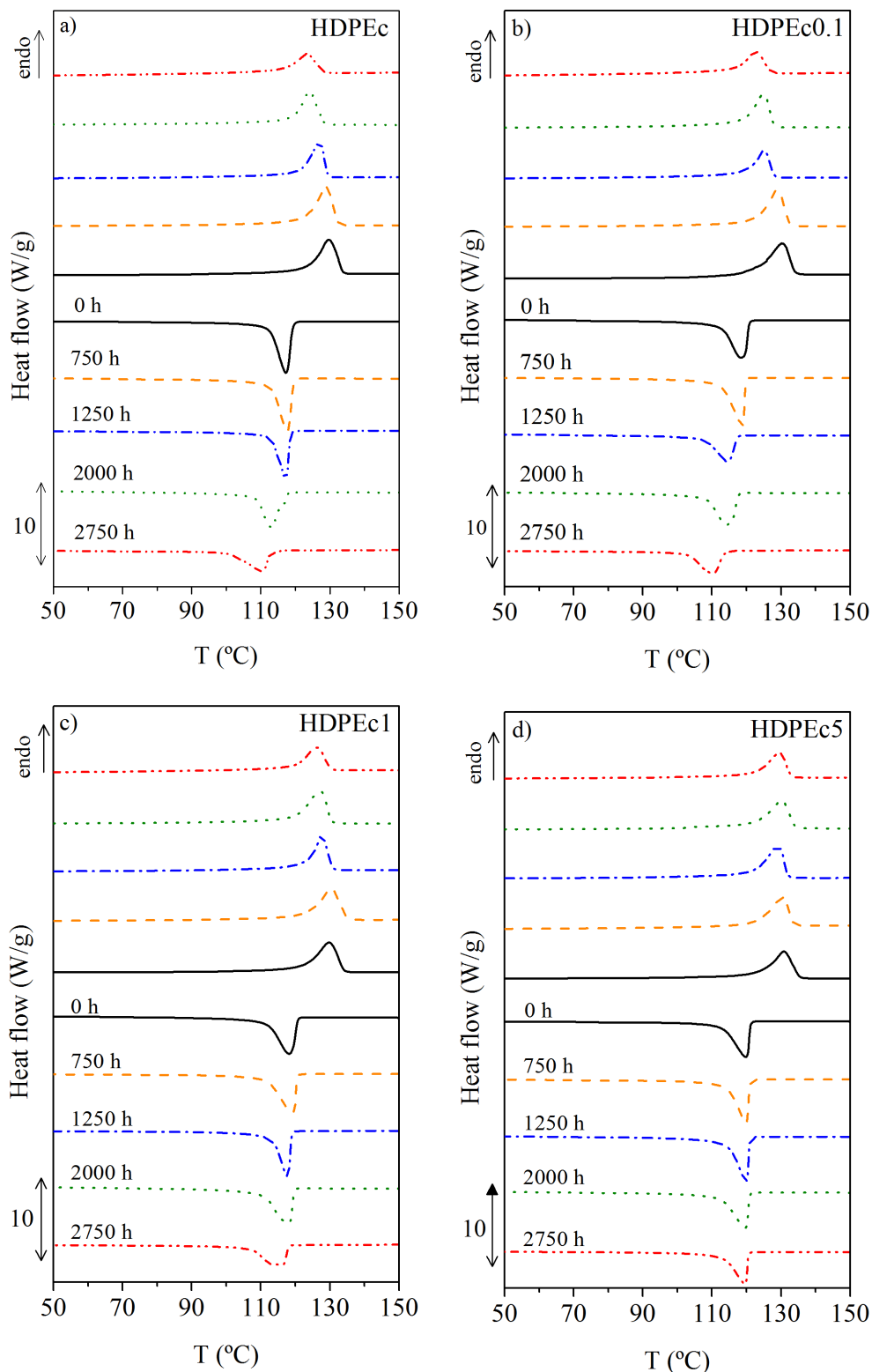


Figure 8 a-d. The variations of the crystallization (T_C) and melting (T_M) temperatures caused by photo-degradation are respectively shown in **Figures 9** and **10**, respectively.

The crystallization temperature (T_C) significantly shifted to lower temperatures the longer the photo-irradiation was. HDPE exposed to long UV/VIS photo-irradiation underwent complex degradation mechanisms in which not only a shortening of macromolecules happened, but also the formation of additional groups, which may act as defects for the crystallization process shifting the T_C to lower values.⁶⁸⁻⁷³ In particular, as shown in **Figure 9**, after 2750 hours of radiation, the decrease of the T_C for the HDPE/Si composites with 1 and 5 wt.% of Si was lower than that shown by HDPE/Si composites with 0.1 wt.% and without Si.

The changes in the melting temperature (T_M) shown in **Figure 10** depended upon the crystal thicknesses and the increase of chain ends, low molar-mass molecules or the presence of new chemical groups from photo-degradation. For HDPE/Si composites with low content of Si microparticles (0.1 wt.%) and samples without Si, the T_M significantly decreased due to long photo-irradiation. In contrast, for HDPE/Si composites with higher Si content (HDPEc1 and HDPEc5), the T_M was stabilised.

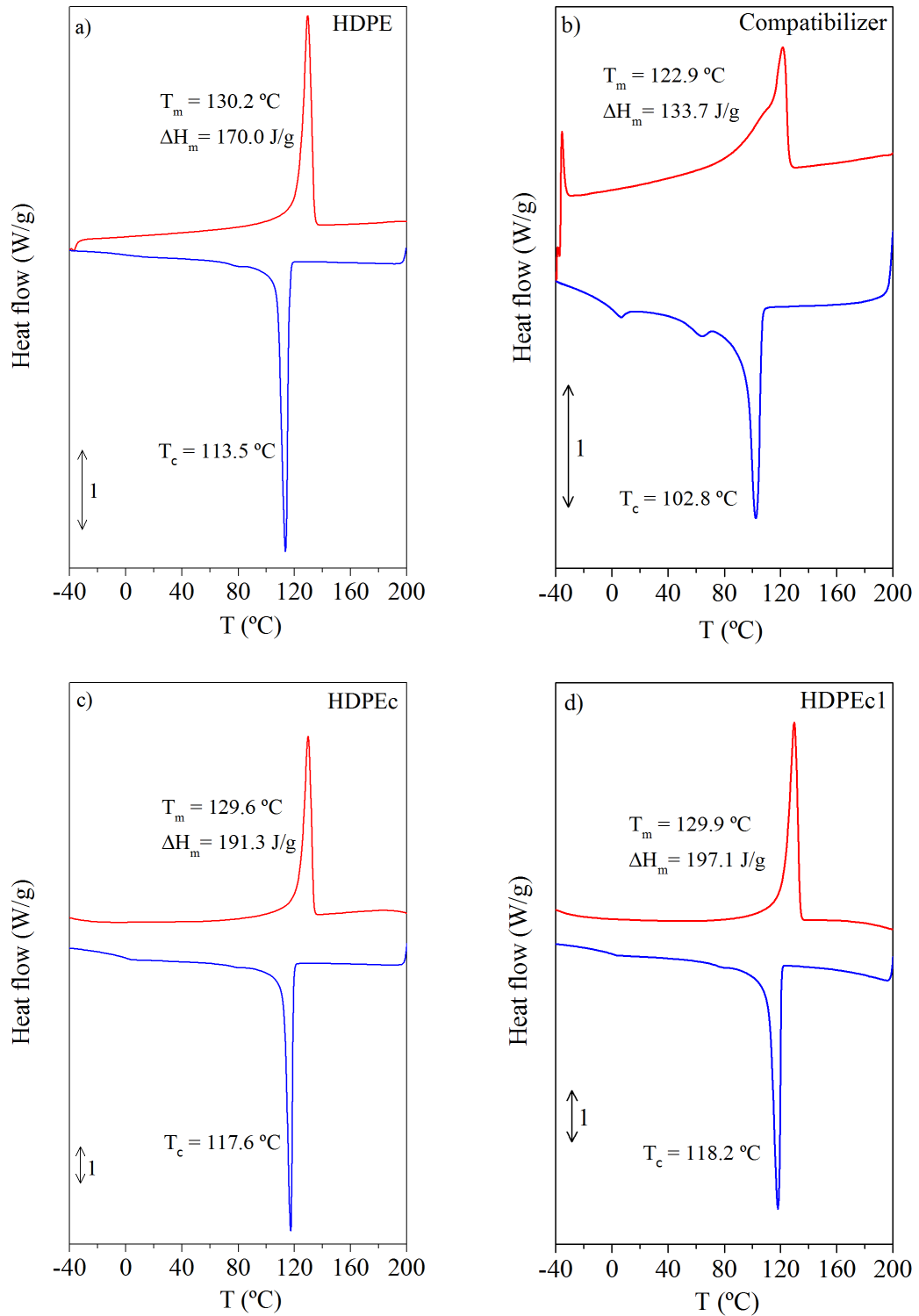


Figure 7. Calorimetric thermograms for a) HDPE, b) coupling agent, c) HDPEc and d) HDPEc1.

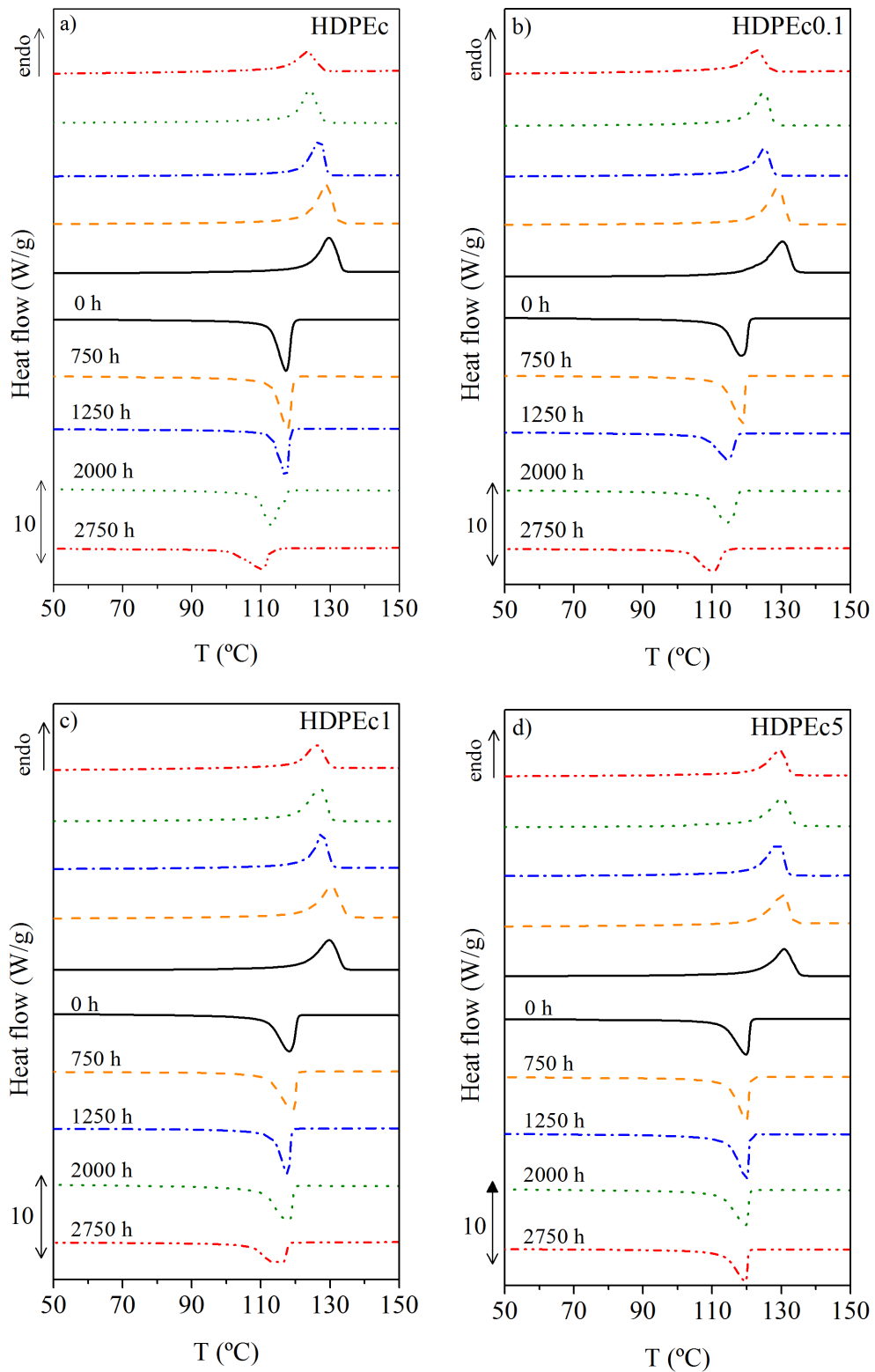


Figure 8. Comparative DSC thermograms of a) HDPEc, b) HDPEc0.1, c) HDPEc1 and d) HDPEc5 exposed to different irradiation times

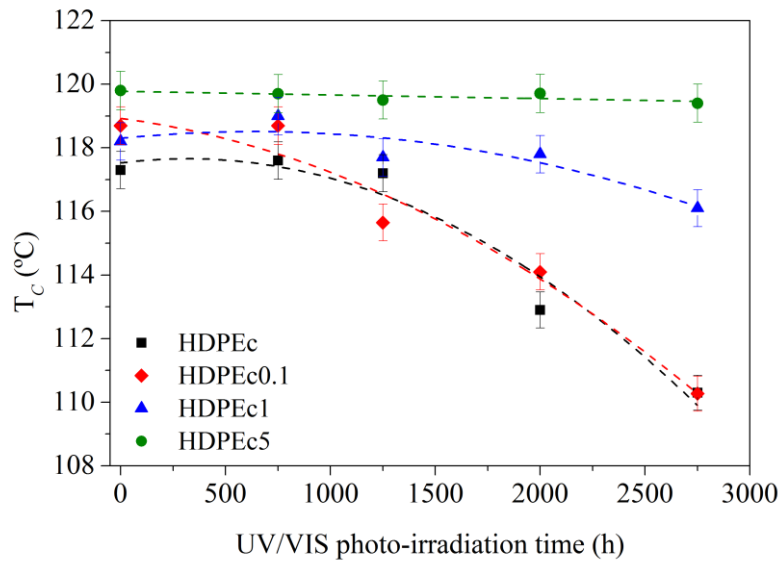


Figure 9. Variation of the crystallization peak temperature of HDPEc/Si composites subjected to UV/VIS photo-irradiation.

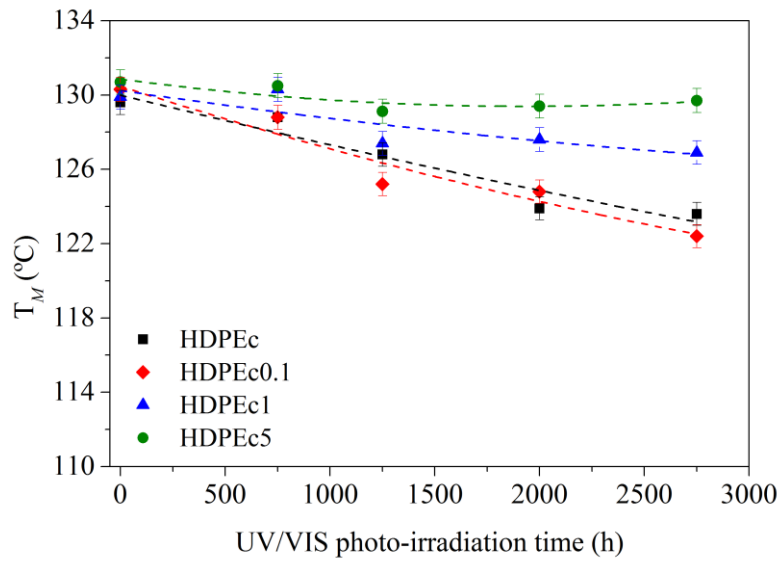


Figure 10. Variation of the melting temperature of HDPEc/Si composites subjected to UV/VIS photo-irradiation

3.6. Influence of Si microparticles on the structural protection of HDPE/Si

composites

In order to establish the structural reason behind the results of stability of HDPEc/Si against photo-irradiation, in contrast to HDPEc, the samples were analysed by Fourier-Transform Infrared Spectroscopy, as shown in **Figure 11 a-d**. To compare the spectra, the area was normalized with respect to the area of the stretching vibration band of the CH₂ groups of the polymer backbone ($\nu \sim 2914$ and 2840 cm^{-1}) as internal reference.

HDPE showed the stretching vibration of the -CH₂- groups of the main chain between 2772 and 3000 cm^{-1} ; and the regions of 1140 - 1490 cm^{-1} and 700 - 750 cm^{-1} corresponding to the vibration of wagging and rocking methylene, respectively.⁷⁴ Photo-irradiation of HDPE followed a Norrish type II degradation mechanism,⁷⁵ which caused a breakage and cross-linking of the polymer chains, the formation of carbonyl -C=O (~ 1620 - 1820 cm^{-1}) and vinyl -CH=CH₂ (~ 1400 - 800 cm^{-1}) groups ⁷⁴ (**Figure 11a**). The increase of these bands was less relevant the higher the amount of Si microparticles was present in the HDPEc/Si composites (**Figure 11 b-d**), particularly blocking the degradation of tertiary carbons of the HDPE backbone preventing from the apparition of vinyl groups.

These results are in agreement with the protective effect observed by indicators as the crystallization, melting temperature peak and the mass-loss of the main decomposition peak. In particular, the HDPEc/Si composites with a 5 wt% of Si microparticles showed the strongest protection, in correlation with the better performance shown by this composite by means of the aforementioned properties.

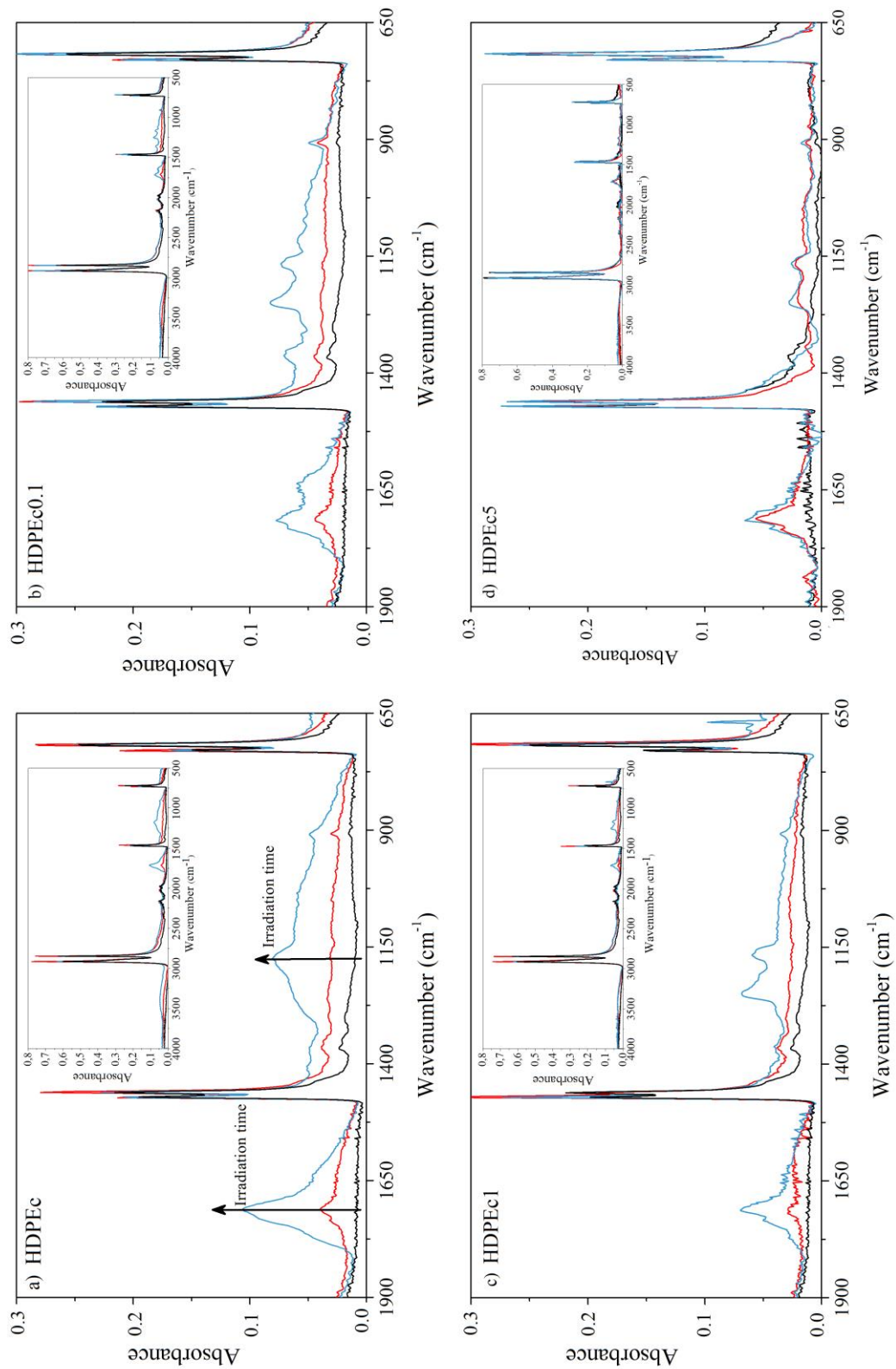


Figure 11 FT-IR spectra of a) HDPEc , b) HDPEc0.1, c) HDPEc1 and d) HDPEc5 subjected to UV/VIS photo-irradiation

4. CONCLUSIONS

The effects of Silicon microparticles to protect HDPE/Si composites from photochemical irradiation was successfully validated by accelerated UV/VIS exposure during up to 2750 h, corresponding to 22 simulated months in outdoor conditions.

The thermo-oxidative decomposition of HDPE, evaluated by thermogravimetry, was prevented by the addition of Si microparticles in the composite, as shown by the increase of the peak decomposition temperature and the reduction of the mass-loss in the low temperature stage.

The crystallization and melting temperatures of HDPE, analysed by differential scanning calorimetry, were kept more invariable the higher the amount of Si microparticles was present. This was specially relevant after a loading of 1 wt.% of Si in the composites, and completely retained for HDPEc/Si with a 5 wt.% of Si microparticles.

The strong light scattering properties of the silicon microparticles, and therefore the shielding of the photo-irradiation on the HDPEc/Si composite, leads to a protective effect of the polymer, avoiding therefore the chain breakage and the formation of vinyl groups, as shown by infrared analysis.

In general terms, the formulation of HDPE/Si composites with a 5 wt.% of Si microparticles was useful to protect polyethylene from photochemical degradation up to 22 months of simulated real exposure.

ACKNOWLEDGMENTS

Funding of this work by European Regional Development Funds and the Spanish Ministry of Economy and Competitiveness is acknowledged through the Research Projects ENE2014-53734-C2-1-R, MAT2012-35040. S. Sánchez-Ballester appreciates the FPI-BES 2012-055316 pre-doctoral grant. Generalitat Valenciana is thanked for the PROMETEOII/2014/026, APOSTD/2013/036 for L. Santonja-Blasco and APOSTD

2014/041 for J.D. Badia. Universitat Politècnica de València is also thanked for the support through the PAID-06-SP20120581 project. The authors would like to acknowledge Puerto Asensio Bros from Inyección de Plásticos ~~Company in~~ (Bocairent, Valencia, Spain) for kindly supplying the polymer, and Dr. L. Cabedo from Jaume I University ~~in~~ (Castelló, Spain) for providing technical assistance with the preparation of samples. Finally, the authors thank the support given by the Electron Microscopy Service of Universitat Politècnica de València.

REFERENCES

1. Plastics Europe, “Plastics—the Facts 2014/2015 An analysis of European plastics production, demand and waste data,” *Plast. Eur.* Brussels Google Sch., **2015**.
2. Vasile, C. *Handbook of polyolefins*. CRC Press, **2000**
3. Rabek, J. F. *Polymer Photodegradation: Mechanisms and Experimental Methods*. New York, NY Chapman Hall, **1995**.
4. Wiles, D. M.; Scott, G. *Polym. Degrad. Stab.* **2006**, *91*, 1581–1592.
5. Andrady, A. L. Degradation of Plastics in the Environment, in *Plastics and Environmental Sustainability*, John Wiley & Sons, Inc, **2015**, pp. 145–184.
6. Taylor, L. J.; Tobias, J. W. *J. Appl. Polym. Sci.* **1981**, *26*, 2917–2926.
7. Morancho, J. M.; Ramis, X.; Fernández, X.; Cadenato, A.; Salla, J. M.; Vallés, A.; Contat, L.; Ribes, A. *Polym. Degrad. Stab.* **2006**, *91*, 44–51.
8. Gugumus, F. *Macromol. Mater. Eng.* **1990**, *182*, 111–134.
9. Rabek, J. F. *Photostabilization of Polymers: Principles and Application*. Springer Science & Business Media, **2012**.
10. Carlsson, D. J.; Wiles, D. M. *J. Macromol. Sci. Macromol. Chem.* **1976**, *14*, 65–106.
11. Horrocks, A. R.; D’Souza, J. A.; Hamid, S. H.; Amin, M. B.; Maadhah, A. G. *Handbook of Polymer Degradation*, Hamid, S.H; Amin, M. B.; Maadhah, A.G. Eds. Marcel Dekker, New York, **1992**.
12. Sampers, J. *Polym. Degrad. Stab.* **2002**, *76*, 455–465.
13. Santonja-Blasco, L.; Ribes-Greus, A.; Alamo, R. G. *Polym. Degrad. Stab.* **2013**, *98*, 771–784.
14. Saenz de Juano, V.; Ribes-Greus, A. *Polimery.* **2009** *54*, 250–254.
15. Badia, J. D.; Gil-Castell, O.; Ribes-Greus, A. *Polym. Degrad. Stab.* **2017**, *137*, 35–57.
16. Griffini, G.; Turri, S. *J. Appl. Polym. Sci.* **2016**, *133*, 43080
17. Bodaghi, H.; Mostofi, Y.; Oromiehie, A.; Ghanbarzadeh, B.; Hagh, Z. G. *J. Appl. Polym. Sci.* **2015**, *132*, 41764.
18. Busolo, M. A.; Lagaron, J. M. *Food Packag. Shelf Life*, **2015**, *6*, 30–41.
19. Oluz, Z.; Tinçer, T. *J. Appl. Polym. Sci.* **2016**, *133*, 43354.
20. Yang, H.; Zhu, S.; Pan, N. *J. Appl. Polym. Sci.* **2004**, *92*, 3201–3210.
21. Li, R.; Yabe, S.; Yamashita, M.; Momose, S.; Yoshida, S.; Yin, S.; Sato, T. *Mater. Chem. Phys.* **2002**, *75*, 39–44.

22. Zhao H.; Li, R. K. Y. *Polymer* **2006**, *47*, 3207–3217.
23. Moustaghfir, A.; Rivaton, A.; Tomasella, E.; Mailhot, B.; Cellier, J.; Jacquet, M.; Gardette, J. *J. Appl. Polym. Sci.* **2005**, *95*, 380–385.
24. Bigger, S. W.; Delatycki, O. *J. Mater. Sci.* **1989**, *24*, 1946–1952.
25. Gugumus, F. *Polym. Degrad. Stab.* **1991**, *34*, 205–241.
26. Gijsman, P.; Hennekens, J.; Tummers, D. *Polym. Degrad. Stab.* **1993**, *39*, 225–233.
27. Klemchuk, P. P.; Gande, M. E.; Cordola, E. *Polym. Degrad. Stab.* **1990**, *27*, 65–74.
28. Muniyandi, S. K.; Sohaili, J.; Hassan, A. *J. Appl. Polym. Sci.* **2016**, *133*, 43110.
29. Fenollosa, R.; Meseguer, F.; Tymczenko, M. *Adv. Mater.* **2008**, *20*, 95–98.
30. Esteve R. F.; Rico, F. J. M.; Tymczenko, M. Silicon microspheres and photonic sponges, production process and their applications. Patent US20100282321 A1, **2010**.
31. Gupta, K. K.; Tripathi, V. S.; Ram, H.; Raj, H. *Colourage*, **2002**, *49*, 35–40.
32. Rodriguez, I.; Fenollosa, R.; Meseguer, F. *Cosmet. Toilet.* **2010**, *125*, 42–50.
33. Fenollosa Esteve, R.; Meseguer, F.; Pérez-Roldán, A.; Rodriguez, M.-I. Photoprotective composition against uv/vis/ir radiation with silicon microspheres as an active compound, Patent WO2011092368, **2011**.
34. Rodriguez, M.-I.; Fenollosa Esteve, R.; Meseguer Rico, J. Formulation comprising silicon microparticles, as a pigment that can absorb visible UV radiation and reflect IR radiation, Patent WO2012101306, **2012**.
35. Badia, J. D.; Santonja-Blasco, L.; Moriana R.; Ribes-Greus A. *Polym. Degrad. Stab.* **2010**, *95*, 2192–2199.
36. Santonja-Blasco, L.; Moriana, R.; Badia, J. D.; Ribes-Greus, A. *Polym. Degrad. Stab.* **2010**, *95*, 2185–2191.
37. Badia, J. D.; Vilaplana, F.; Karlsson, S.; Ribes-Greus A. *Polym. Test.* **2009**, *28*, 169–175.
38. da Costa, H. M.; Ramos, V. D.; de Oliveira, M. G. *Polym. Test.* **2007**, *26*, 676–684.
39. Aoyagi, Y.; Yamashita, K.; Doi, Y. *Polym. Degrad. Stab.* **2002**, *76*, 53–59.
40. Badia, J. D.; Martinez-Felipe, A.; Santonja-Blasco, L.; Ribes-Greus, A. *J. Anal. Appl. Pyrolysis*, **2013**, *99*, 191–202.
41. Gil-Castell, O.; Badia, J. D.; Teruel-Juanes, R.; Rodriguez, I.; Meseguer, F.; Ribes-Greus, A. *Eur. Polym. J.* **2015**, *70*, 247–261.
42. E. N. ISO, “4892-2 (2006) Plastics,” Methods Expo. to Lab. Light sources. Part, vol. 2.
43. Robinson, J.; Linder, A.; Gemmel, A.; Poulsen, K. V.; Burkhard, H.; Högrström, P.-A.; Kobilsek, M. Comparison of standard UV test method for the ageing of cables, In Proceedings of the 60th International Wire & Cable Symposium, **2011**, pp. 329–337.
44. ISO 11358:2014 Plastics -- Thermogravimetry (TG) of polymers
45. ISO 11357:2016 Plastics -- Differential scanning calorimetry (DSC)
46. Hummel, D. O. Atlas of plastics additives: analysis by spectrometric methods. Springer Science & Business Media, **2012**.
47. Bula, K.; Jesionowski, T. *Compos. Interfaces* **2010**, *17*, 603–614.
48. Liu, W.; Wang, Y.; Sun, Z. *J. Appl. Polym. Sci.* **2003**, *88*, 2904–2911.
49. Villanueva, M. P.; Cabedo, L.; Lagarón, J. M.; Giménez, E. *J. Appl. Polym. Sci.* **2010**, *115*, 1325–1335.
50. Morisaki, S. *Thermochim. Acta* **1974**, *9*, 157–169.
51. Costa, L.; Luda, M. P.; Trossarelli, L. *Polym. Degrad. Stab.* **1997**, *55*, 329–338.
52. Lacoste, J.; Carlsson, D. J.; Falicki, S.; Wiles, D. M. *Polym. Degrad. Stab.* **1991**, *34*, 309–323.
53. Gedde, U. W.; Jansson, J.-F. *Polym. Test.* **1980**, *1*, 303–312.

54. Tiwari, A.; Raj, B. Reactions and mechanisms in thermal analysis of advanced materials. John Wiley & Sons, **2015**.
55. Moriana-Torró, R.; Contat-Rodrigo, L.; Santonja-Blasco, L.; Ribes-Greus, A. *J. Appl. Polym. Sci.* **2008**, *109*, 1177–1188.
56. Camacho W.; Karlsson, S. *Polym. Degrad. Stab.* **2002**, *78*, 385–391.
57. Badia, J. D.; Santonja-Blasco, L.; Martínez-Felipe, A.; Ribes-Greus, A. *Bioresour. Technol.* **2012**, *111*, 468–475.
58. Badia, J. D.; Santonja-Blasco, L.; Martínez-Felipe, A.; Ribes-Greus, A. *Bioresour. Technol.* **2012**, *114*, 622–628.
59. Badia, J. D.; Strömberg, E.; Karlsson, S.; Ribes-Greus, A. *Polym. Degrad. Stab.* **2012**, *97*, 98–107
60. Badia, J. D.; Strömberg, E.; Karlsson, S.; Ribes-Greus, A. *Polym. Degrad. Stab.* **2012**, *97*, 670–678.
61. Badia, J. D.; Santonja-Blasco, L.; Martínez-Felipe, A.; Ribes-Greus, A. *Polym. Degrad. Stab.* **2012**, *97*, 1881–1890.
62. Gil-Castell, O.; Badia, J. D.; Strömberg, E.; Karlsson, S.; Ribes-Greus, A. *Eur. Polym. J.* **2017**, *87*, 174–187.
63. Badia, J.D.; Ribes-Greus, A. *Eur. Polym. J.* **2016**, *84*, 22-39.
64. Gil-Castell, O.; Badia, J.D.; Kittikorn, T.; Strömberg, E.; Martínez-Felipe, A.; Ek, M.; Karlsson, S.; Ribes-Greus, A. *Polym. Degrad. Stab.* **2014**, *108*, 212-222.
65. Badia, J.D.; Strömberg, E.; Karlsson, S.; Ribes-Greus A. *Polym. Degrad. Stab.* **2012**, *97*, 670-678.
66. Jiasheng, Q.; Pingsheng, H. *J. Mater. Sci.* **2003**, *38*, 2299-2304.
67. Seven, K. M.; Cogen, J. M.; Gilchrist, J. F. *Polym. Eng. Sci.* **2016**, *56*, 541–554.
68. Peacock, A. Handbook of polyethylene – structures, properties and applications. Marcel Dekker, New York, Basel **2000**.
69. Hamid, S. H.; Amin, M. B. *J. Appl. Polym. Sci.* **1995**, *55*, 1385–1394.
70. Janimak, J. J.; Cheng, S. Z. D.; Giusti, P. A.; Hsieh, E. T. *Macromolecules* **1991**, *24*, 2253–2260.
71. Gulmine, J. V.; Janissek, P. R.; Heise, H. M.; Akcelrud, L. *Polym. Degrad. Stab.* **2003**, *79*, 385–397.
72. Mandelkern, L. Crystallization of Polymers: Volume 1, Equilibrium Concepts. Cambridge University Press, **2002**.
73. Mandelkern, L. Crystallization of Polymers: Volume 2, Kinetics and Mechanisms. Cambridge University Press, **2004**.
74. Wypych, G. Handbook of material weathering. Chem-Tec Publ. Toronto. 2003.
75. Rabek, J. F. Photochemical aspects of degradation of polymers, In Polymer photodegradation, Springer, **1995**, pp. 24–66.

ANNEX. OPEN ACCESS POLICIES

The screenshot displays the SHERPA/RoMEO website interface. At the top, the SHERPA/RoMEO logo is on the left, and the tagline "... opening access to research" is on the right. Below the logo, there are navigation links: Home, Search, Journals, Publishers, FAQ, Suggest, and About. The main heading is "Search - Publisher copyright policies & self-archiving", with language options: English, Español, Magyar, Nederlands, and Português.

The search results show one journal found: "Journal of Applied Polymer Science" (ISSN: 0021-8995, EISSN: 1097-4628). The RoMEO status is "yellow". The "Paid OA" status is "A paid open access option is available for this journal".

Author's Pre-print: ✓ author can archive pre-print (ie pre-refereeing)
Author's Post-print: ✓ subject to Restrictions below, author can archive post-print (ie final draft post-refereeing)

Restrictions:
• 12 months embargo

Publisher's Version/PDF: ✗ author cannot archive publisher's version/PDF

General Conditions:
• Some journals have separate policies, please check with each journal directly
• On author's personal website, institutional repositories, arXiv, AGEcon, PhilPapers, PubMed Central, RePEc or Social Science Research Network
• Author's pre-print may not be updated with Publisher's Version/PDF
• Author's pre-print must acknowledge acceptance for publication
• Non-Commercial
• Publisher's version/PDF cannot be used
• Publisher source must be acknowledged with citation
• Must link to publisher version with set statement (see policy)
• If OnlineOpen is available, BBSRC, EPSRC, MRC, NERC and STFC authors, may self-archive after 12 months

Mandated OA: (Awaiting information)
Paid Open Access: [OnlineOpen](#)

Notes:
• Publisher last contacted on 07/06/2014

Copyright: [Self-archiving - Authors Compliance Tool - Funder Policies](#)
Updated: 24-Nov-2017 - [Suggest an update for this record](#)

Link to this page: <http://www.sherpa.ac.uk/romeo/issn/0021-8995/>

Published by: Wiley: 12 months [Commercial Publisher] - [Yellow Policies in RoMEO](#)
For: [Wiley Periodicals](#) [imprint]

Guidance: Please see the list of [Publisher Categories in RoMEO](#) for guidance on interpreting the priority of multiple publishers.

These summaries are for the journal's **default** policies, and changes or exceptions can often be negotiated by authors.
All information is correct to the best of our knowledge but should not be relied upon for legal advice.